NASA Technical Memorandum 87119

# Ion Beam Sputter Deposited Zinc Telluride Films



Daniel A. Gulino
*Lewis Research Center*
*Cleveland, Ohio*


Prepared for the
32rd National Symposium of the American Vacuum Society
Houston, Texas, November 18-22, 1985

NASA

# ION BEAM SPUTTER DEPOSITED ZINC TELLURIDE FILMS

Daniel A. Gulino
National Aeronautics and Space Administration
Lewis Research Center
Cleveland, Ohio 44135

## ABSTRACT

Zinc telluride is of interest as a potential electronic device material, particularly as one component in an amorphous superlattice, which is a new class of interesting and potentially useful materials. This paper describes some structural and electronic properties of ZnTe films deposited by argon ion beam sputter deposition. Films (up to 3000 Å thick) were deposited from a ZnTe target. A beam energy of 1000 eV and a current density of 4 $mA/cm^2$ resulted in deposition rates of approximately 70 Å/min. The optical band gap was found to be approximately 1.1 eV, indicating an amorphous structure, as compared to a literature value of 2.26 eV for crystalline material. Intrinsic stress measurements showed a thickness dependence, varying from tensile for thicknesses below 850 Å to compressive for larger thicknesses. Room temperature conductivity measurements also showed a thickness dependence, with values ranging from $1.86 \times 10^{-6}$ $\Omega^{-1}$ $cm^{-1}$ for a 300 Å film to $2.56 \times 10^{-7}$ $\Omega^{-1}$ $cm^{-1}$ for a 2600 Å film. Measurement of the temperature dependence of the conductivity for these films showed complicated behavior which was thickness dependent. Thinner films showed at least two distinct temperature dependent conductivity mechanisms, as described by a Mott-type model. Thicker films showed only one principal conductivity mechanism, similar to what might be expected for a material with more crystalline character.

E-2726

## INTRODUCTION

In recent years there has been interest in the properties of amorphous II-VI compounds, including amorphous zinc telluride (a-ZnTe) (Refs. 1 to 5). Thin films of these materials deposited by vacuum evaporative techniques have

been shown to be essentially amorphous, with microcrystallite sizes less than 20 Å in any direction. As-deposited a-ZnTe has been found to be stable essentially indefinitely at room temperature, with crystallization times on the order of 100 yr (Ref. 6). These films exhibit electrical conductivity consistent with a Mott-type model in which conduction in extended states above the band edges dominates at high temperatures, and conduction by hopping in band tail states and states near the Fermi level becomes dominant at lower temperatures. Investigators have also prepared an a-ZnSe/a-ZnTe heterojunction which exhibits diode-like behavior (Refs. 7 to 9).

It is this last discovery which motivates the work to be described here. The field of amorphous semiconductor superlattices is relatively new, with much of the work to date having been done at Exxon, the University of Chicago, and the University of Arizona (Refs. 10 to 14) as well as in Japan (Ref. 15). The research has been primarily concerned with preparing and characterizing amorphous silicon and silicon compounds, particularly silicon carbide and silicon nitride. The materials investigated exhibit a number of the properties of crystalline superlattices, even though the condition of registry at the interfaces is relaxed. These findings open up a whole new field of exploration with regard to amorphous semiconductors and may make possible new device materials.

This paper reports an investigation of some structural, optical, and electrical properties of ZnTe films prepared by ion beam sputter deposition, with an eye toward potential use in a superlattice structure. It also compares films prepared in this way to those prepared by evaporative techniques.

## APPARATUS AND PROCEDURE

Thin films (300 to 3000 Å thick) of ZnTe were fabricated by sputtering a pressed powder target of this material with an argon ion beam onto 2 cm square,

fused silica substrates mounted on a water-cooled holder. An Ion Tech® Dual Beam sputtering system, which contained both a 2.5 and a 15 cm ion source (see Fig. 1), was used to deposit the films. The target, 12.7 cm in diameter and 0.64 cm thick, was mounted on the cube-shaped holder, which was also water cooled. The substrates were mounted with polyimide Kapton® tape onto the substrate holder. Special masks over portions of the substrates permitted deposition of the films in a bridge-shaped configuration (see Fig. 2), which facilitated subsequent resistance measurements. Other samples deposited over the whole substrate were used for other resistance measurements and for optical measurements. The source-to-target distance was 20.3 cm, and the target-to-substrate distance was 15.3 cm (see Fig. 3). Argon ion beam energies during deposition were 1000 eV, and beam current densities were approximately 3.5 $mA/cm^2$. Film thicknesses and hence the deposition rate were measured using a Tencor®Alpha-Step profile measuring system. The deposition rate was ~70 Å/min for ZnTe at these beam conditions.

The second argon ion source in this system permitted ion beam cleaning of the substrate surfaces immediately prior to deposition. Prior cleaning of a substrate in this way has been shown to greatly improve the adherence of sputter deposited films (Ref. 16). For this work, all substrates were precleaned for 2 min with a 250 eV, 0.17 $mA/cm^2$ ion beam at a 45° angle of incidence.

Intrinsic stress measurements were performed using an Ionic Systems® stress gauge. For these measurements, films were deposited onto ion beam-cleaned silicon wafers 7.6 cm in diameter.

The optical band gap, $E_g$, was measured using a Perkin-Elmer® Lambda-9 spectrophotometer. Spectral absorptances ($\alpha_\lambda$) were calculated from total transmittance ($t_\lambda$) and total reflectance ($\rho_\lambda$) curves [$\alpha_\lambda = 1 - (\rho_\lambda + t_\lambda)$] and plotted as $(\alpha_\lambda E)^{1/2}$ versus E. The straight line portion of

the graph was extrapolated to $(\alpha_\lambda E)^{1/2} = 0$ and this intercept taken as $E_g$ (Ref. 17).

Electrical contact to the films was accomplished with the same deposition system by masking all but the arms of the bridge-shaped samples and sputtering from a gold target. The shape of the deposited films permitted a four-point measurement of resistance. Currents were provided by a Keithley® Model 225 current source or a Keithley® Model 616 electrometer operated as a current source. In either case, voltages were measured using a second Keithley® 616. Cryogenic temperatures for these measurements were obtained with an Air Products Displex closed cycle helium refrigeration system operated in the range of 40 to 300 K.

Room temperature resistivity measurements were performed on films which covered the entire substrate. Gold contacts were sputtered onto the films in a gap configuration. The gap was approximately 1 mm. For these measurements, a single Keithley 616 was used to measure resistance.

## RESULTS AND DISCUSSION

### General Visual Observations

Zinc telluride films (300 to 3000 Å thick) deposited by ion beam sputter deposition appeared smooth, shiny, and translucent with a dark amber color. These as-deposited films did not spall, crack, or show any other outward signs of stress or poor adhesion. Evaporated zinc telluride films have been reported to be stable upon deposition, with crystallization times on the order of 100 yr (Ref. 6).

### Intrinsic Stress

The results of the intrinsic stress measurements are shown in Fig. 4, which depicts intrinsic stress versus film thickness. Two regions are observed, with thinner films under tensile stress and thicker films under compressive stress. The data point at zero thickness is, of course, not an

actual measurement of a ZnTe film, but is the measured stress on a silicon wafer which has been subjected only to the ion beam cleaning procedure. This data point shows that this cleaning procedure does not itself introduce any measureable stress to the silicon wafer prior to film deposition.

The transition from tensile to compressive stress suggests that, in thinner films, stress is dominated by properties of the film/substrate interface, while in thicker films, it is dominated by properties of the growing bulk film. Chopra (Ref. 18) reviewed the properties of thin films, and he discussed several models for the origin of intrinsic stress. According to his discussion, a surface tension effect may explain the behavior observed here. Initially, the film consists of isolated islands of ZnTe, each tending to coalesce with those nearby and thus causing the tensile stress. At the same time, a compressive stress is caused by the inability of these individual islands to spread out to cover the surface. This stress arises from the attempt by an island to accommodate later arriving material by increasing in surface area, rather than by increasing in thickness. For very thin films, the tensile component dominates, as is observed. As the film becomes thicker, the islands coalesce and their number decreases, thus reducing the tensile component. At some thickness the two effects balance, and the net stress is zero. The compressive component then begins to dominate as thickness is increased further.

The shape of the curve in Fig. 4 suggests that the stress approaches a constant value for films greater than 3000 Å thick. While more data is needed to confirm this, other work (Ref. 19) on a large number of materials has shown this to be the general case for thick, continuous metal and semiconductor films.

## Optical Band Gap

Figure 5 shows the optical properties of total transmittance, total reflectance, and absorptance for a 1000 Å thick film as a function of wavelength between 400 and 1000 nm. A plot of $(\alpha_\lambda E)^{1/2}$ versus E, as shown in Fig. 5, gives an E intercept (equal to $E_g$, the optical band gap) of 1.12 eV. This value differs markedly from the crystalline value of 2.26 eV. It also differs markedly from the value of 2.35 eV reported by Brown and Brodie (Ref. 20), whose samples were prepared by evaporative techniques. Their samples were annealed in helium for several hours at high temperatures (350 °C), which apparently crystallizes them.

In an attempt to determine if annealing has any effect on these samples, a second, identical ZnTe film was subjected to a 2 hr anneal at 100 °C at $10^{-4}$ torr. While these conditions were not identical to those described in Ref. 20, one might reasonably expect some effect on $E_g$. A second series of spectra was obtained (Fig. 7). The result is that $E_g$ was unchanged (Fig. 8).

Figure 9 shows a comparison of the absorptance curves before and after annealing for the same sample. As can be seen, there is a very small shift of the absorption edge to longer wavelengths. The conclusion is that annealing under these conditions does not appreciably affect $E_g$. While a higher temperature anneal, such as was used by Brown and Brodie, might have an effect, it is difficult to imagine that a change in $E_g$ as large as 1 eV would occur.

A value of $E_g$ below the crystalline value is not surprising, considering the amorphous nature of these films. The disruption of the periodicity of the crystalline structure would be expected to result in a significant increase in both the conduction and valence band tail states, lowering the effective optical band gap. Additional experimentation is needed

to determine if anneal conditions could be found which would result in crystallization of these films.

## Conductivity

The conductivities of these ZnTe films were measured both as a function of film thickness and temperature. Figure 10 shows the thickness dependence for as-deposited films measured using the gap configuration. The conductivity decreases with increasing thickness, with values ranging from $1.86 \times 10^{-6}$ $\Omega^{-1}$ $cm^{-1}$ for a 300 Å film to $2.56 \times 10^{-7}$ $\Omega^{-1}$ $cm^{-1}$ for a 2600 Å film.

Figure 11 is a plot of the conductivity versus temperature over the range 40 to 300 K for as-deposited films of three different thicknesses. The most interesting feature in the figure is the thickness dependence of the three plots. For the thinnest film (1300 Å), the conductivity decreases rapidly as the temperature is lowered to about 125 K, and then is approximately constant between 125 and 40 K. As the film thickness is increased, the room temperature conductivity decreases (consistent with Fig. 10), and only a small decrease in conductivity with decreasing temperature is observed. The thickest film studied (3125 Å) showed very little temperature dependence.

The conductivity of the thinnest film, curve (a), is well represented by a Mott-type model (Ref. 21). In this model, conduction at higher temperatures is accomplished by carrier excitation (holes, in this case, since a-ZnTe is p-type, see Ref. 1) from states near the Fermi level, $E_F$, to extended states in the valence band. This may be represented by Eq. (1)

$$\sigma = \sigma(0)\exp[-(E_F - E_V)/kT] \qquad (1)$$

where $\sigma$ is the conductivity, $E_V$ is the energy of the valence band edge, $k$ is Boltzmann's constant, and $T$ is the absolute temperature. A plot of $\ln \sigma$ versus $1/T$ should be linear, as is observed. The calculated activation energy (equal to $-E_F + E_V$) is 0.210 eV. At low temperatures,

conduction results from hopping between localized states in the defect band near the Fermi level. This may be represented by Eq. (2)

$$\sigma_2 = \sigma_2(0)\exp[-E_2/kT] \qquad (2)$$

where $E_2$ is the activation energy for hopping conduction in the defect band. Here the activation energy ($E_2$) is found to be 0.00132 eV. At intermediate temperatures, according to the Mott model, conduction arises by carrier excitation from states near the Fermi level to localized states in the valence band. This may be represented by Eq. (3)

$$\sigma_1 = \sigma_1(0)\exp[-(E_F - E_B + E_{HOP})/kT] \qquad (3)$$

where $E_B$ is the energy of the localized valence band tail, and $E_{HOP}$ is the activation energy for hopping conduction. Here a plot of $\ln \sigma$ versus $1/T$ gives an activation energy (equal to $-E_F + E_B - E_{HOP}$) of 0.00516 eV.

Curve (b) of Fig. 11, which is for a 2000 Å film, shows two distinct conductivity regions and a much sharper "knee" with no easily discernible intermediate temperature conductivity mechanism. Applying the Mott model to this curve, the higher and lower temperature activation energies were found to be 0.131 and 0.00065 eV, respectively.

Curve (c), which is for a 3125 Å film, shows very little variation of conductivity with temperature over the temperature range studied. A linear higher temperature region is just barely discernible, and its activation energy was found to be 0.0264 eV. The activation energy for the lower temperature region was calculated to be 0.000170 eV. If a wider temperature range (to include higher temperatures) could be covered, one would expect both curves (b) and (c) to be similar in shape to curve (a)

Ordinarily, one would expect parameters such as $E_2$, $E_B$, and $E_{HOP}$ to be intrinsic to the material and to be independent of film thickness. In other words, one would expect them to be dependent on the bulk structure of

the film. This would be the case only if the bulk structure itself is independent of film thickness. The results obtained here indicate that this is not true when the film is sufficiently thin.

The trend indicated in Fig. 11 is what might be expected for films which behave with more crystalline character as thickness increases. At higher temperatures, an amorphous semiconductor, with its significant density of states within the gap (see Fig. 2 of Ref. 21), would be expected to have a higher conductivity than a crystalline sample of the same material. As the temperature is lowered, the conductivity would be expected to decrease rapidly as the carriers that exist within the gap lose the thermal energy necessary for excitation. At low temperatures, the conductivity arises only from hopping of the carriers located in the few states at or near the Fermi level. A crystalline semiconductor would have a smaller conductivity at the same high temperature because the density of states within the gap is zero. As the temperature is lowered, the conductivity decreases relatively less, since it was low initially.

Apparently, the relative amorphicity or crystallinity of a ZnTe film depends upon its thickness, at least over the thickness range studied. The thicker the film, the more its properties may be dominated (not surprisingly) by its bulk. A thicker film may more easily relax as it grows during sputter deposition. As the later arriving material loses its energy to the film during collision, earlier material may rearrange to a more periodic and hence lower energy configuration. For even thicker films (3000 to 10 000 Å) one would expect the electrical conductivity to be essentially linear over the entire temperature range studied here. One would also expect less of a dependence of room temperature conductivity on thickness. This already appears to be the case from Fig. 11.

## CONCLUSIONS

As stated initially, the intent of this work was to investigate ion beam sputter deposited zinc telluride as a candidate for use in an amorphous superlattice. For films below about 1000 Å in thickness, the intrinsic stress is less than about $10^9$ dyn/cm$^2$, which is a negligible stress for a film this thin. Hence, ZnTe films prepared in this way may be suitable for use in a superlattice structure, where layer thicknesses for the most part range from 10 to 500 Å. The optical band gap is low, being less than half that of the crystalline value. A similar material with a higher gap, such as amorphous zinc selenide, might work well with ZnTe in the fabrication of superlattices with preselectable band gaps, assuming quantum size effects can be observed. The thickness dependence of the conductivity suggests that amorphous superlattices constructed with a-ZnTe will display interesting electrical behavior. Perhaps particular electrical properties could be preselected by choosing a certain ZnTe layer thickness, in much the same way that optical properties might be preselected. Further investigation of the ZnSe/ZnTe system is required.

## REFERENCES


1. J.B. Webb and D.E. Brodie, Can. J. Phys. 52, 2240 (1974).
2. C.J. Moore, B.S. Bharaj, and D.E. Brodie, Can. J. Phys. 59, 924 (1981).
3. P. Ng, J.B. Webb, and D.E. Brodie, Can. J. Phys. 54, 446 (1976).
4. P.K. Lim and D.E. Brodie, Can. J. Phys. 55, 1512 (1977).
5. A. Yoshikawa, K. Tanaka, S. Yamaga, and H. Kasai, Jap. J. Appl. Phys. 23, L424 (1984).
6. J.B. Webb and D.E. Brodie, Can. J. Phys. 53, 2481 (1975).
7. C.J. Moore and D.E. Brodie, Appl. Phys. Lett. 34, 78 (1979).
8. D.E. Brodie and C.J. Moore, Can. J. Phys. 58, 38 (1980).
9. D.E. Brodie and C.J. Moore, Can. J. Phys. 59, 173 (1981).

10. B. Abeles and T. Tiedje, Phys. Rev. Lett. 51, 2003 (1983).

11. B. Abeles, T. Tiedje, K.S. Liang, H.W. Deckman, H.C. Stasiewski, J. C. Scanlon, and P.M. Eisenberger, J. Non-Cryst. Solids. 66, 351 (1984).

12. T. Tiedje, B. Abeles, P. D. Persans, B. G. Brooks, and G. D. Cody, J. Non-Cryst. Solids. 66, 345 (1984).

13. J. Kakalios, H. Fritzsche, N. Ibaraki, and S.R. Ovshinsky, J. Non-Cryst., Solids. 66, 339 (1984).

14. C.M. Falco, J. Appl. Phys. 56, 1218 (1984).

15. T. Ogino and Y. Mizushima, Jap. J. Appl. Phys. 22, 1647 (1983).

16. M.J. Mirtich, J. Vac. Sci. Technol. 18, 186 (1981).

17. N.F. Mott and E.A. Davis, Electronic Processes in Noncrystalline Materials, (Clarendon, Oxford, 1971), p. 197.

18. K.L. Chopra, Thin Film Phenomena, (McGraw-Hill, New York, 1969).

19. E. Klokholm and B.S. Berry, J. Electrochem. Soc. 115, 823 (1968).

20. H.M. Brown and D.E. Brodie, Can. J. Phys. 50, 2502 (1972).

21. E.A. Davis and N.F. Mott, Philos. Mag. 22, 903 (1970).

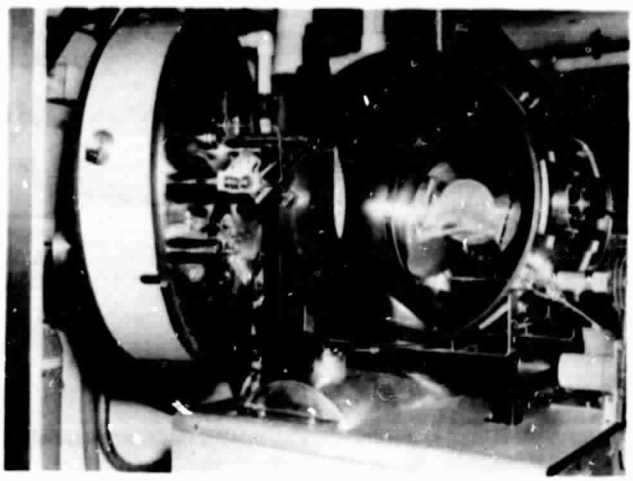

Figure 1. - Photograph of sputtering system, showing target holder (lower right), substrate holder (left of center), 2.5cm ion source (below substrate holder), and 15cm ion source (above target holder).

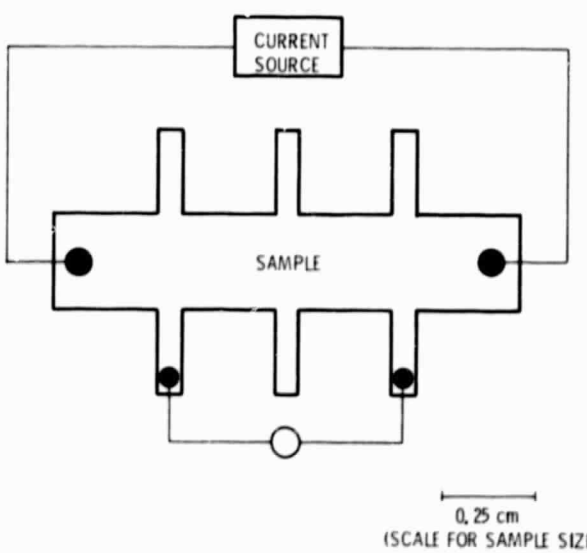


Figure 2. - Sample shape and electronic arrangement for conductivity vs temperature measurements.

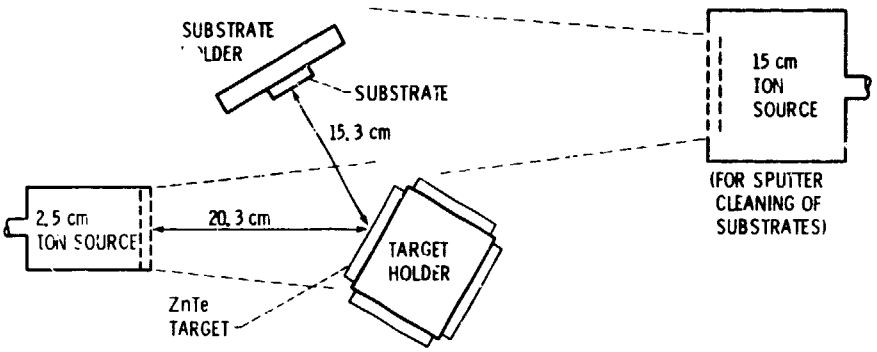


Figure 3. - Schematic diagram of ion beam sputtering apparatus showing spatial arrangement of the ion sources, target holder, and substrate holder.

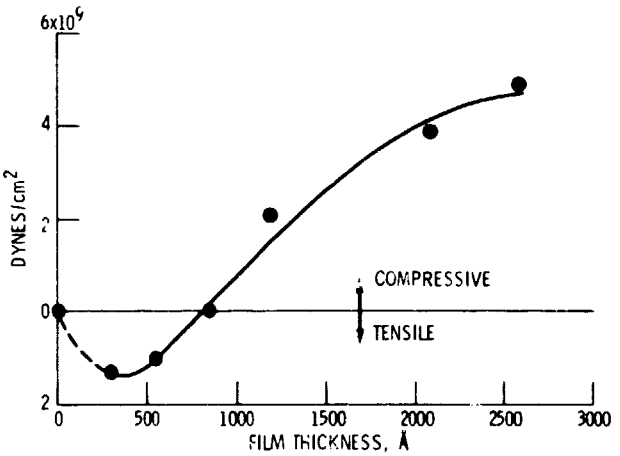


Figure 4. - Intrinsic stress vs film thickness for several thickness of ZnTe films.

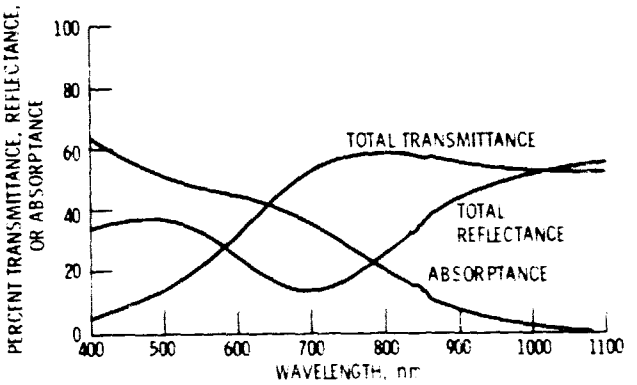


Figure 5. - Transmittance, reflectance, and absorptance curves of an as-deposited ZnTe film 1000 A thick. The absorptance ($\alpha_\lambda$) curve was obtained by summing the transmittance ($t_\lambda$) and reflectance ($\rho_\lambda$) curves and substracting from one. $\alpha_\lambda = [1 - (\rho_\lambda + t_\lambda)]$.

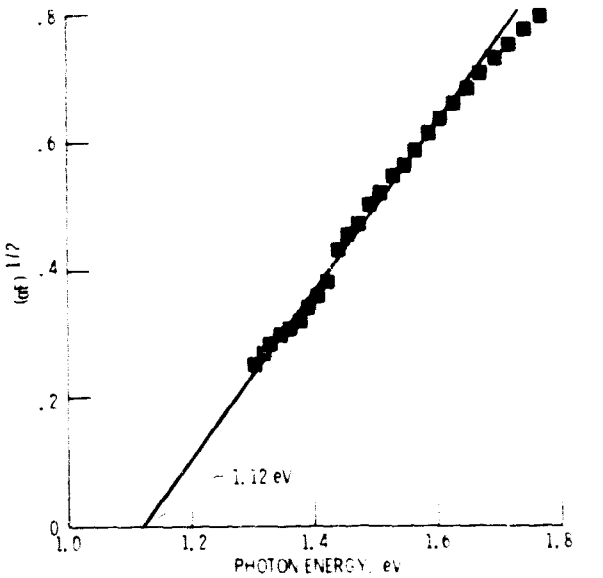


Figure 6. - Plot of $(\alpha_\lambda E)^{1/2}$ vs E for the absorptance curve shown in figure 5. The band gap ($E_G$) is found to be 1.12 eV.

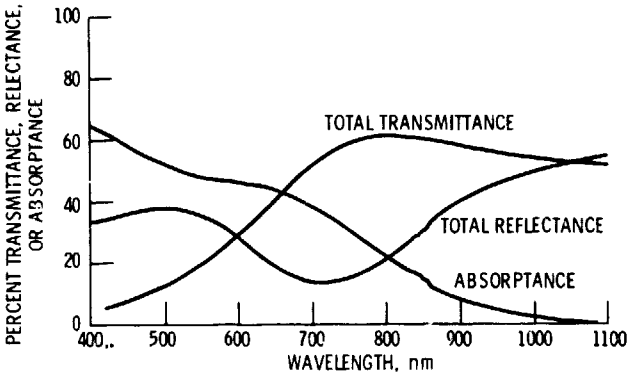


Figure 7. - Transmittance, reflectance, and absorptance curves for a 1000 Å thick ZnTe film on $SiO_2$ after a two hour anneal at 100 °C.

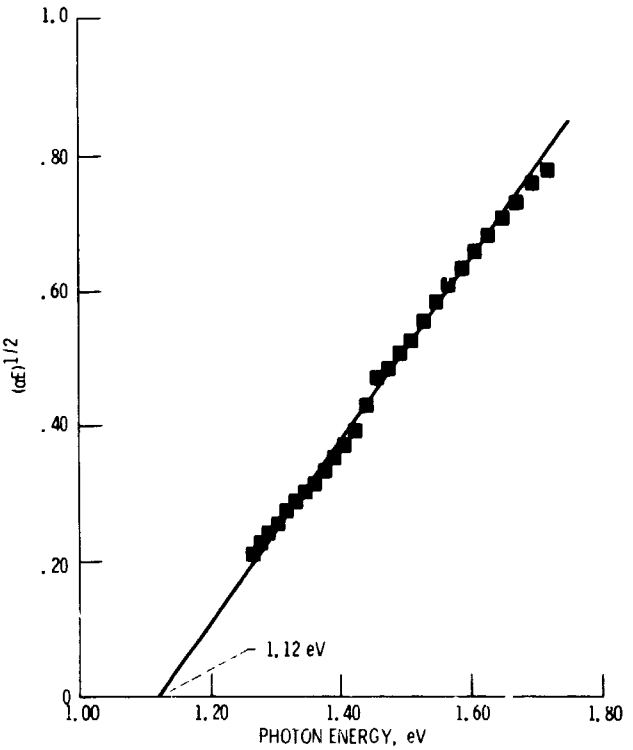


Figure 8. - Plot of $(\alpha_\lambda E)^{1/2}$ vs E for the absorptance curve shown in figure 7. The band gap ($E_g$) is found to be 1.12 eV.

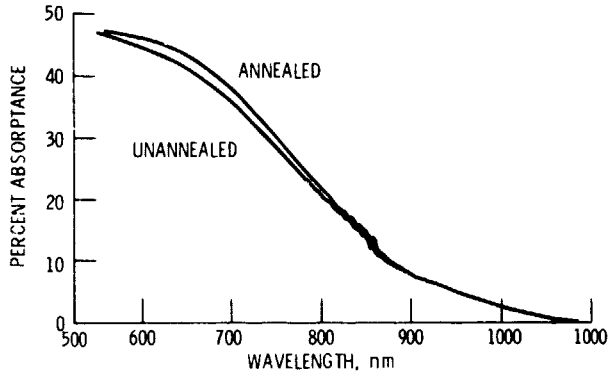


Figure 9. - Comparison of the absorptance curves obtained on a ZnTe film immediately after deposition and then again immediately following anneal.

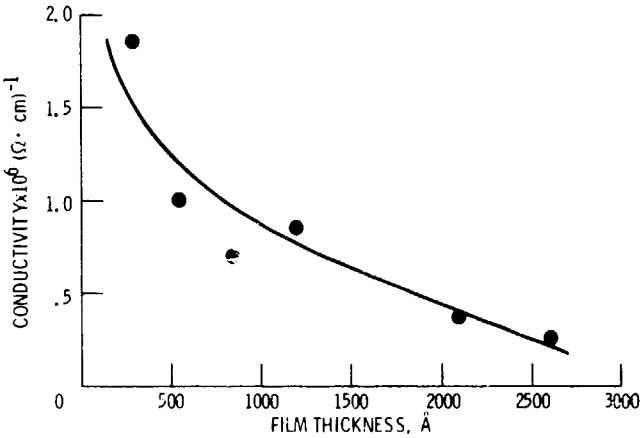


Figure 10. - Room temperature conductivity vs film thickness for several as-deposited ZnTe films.

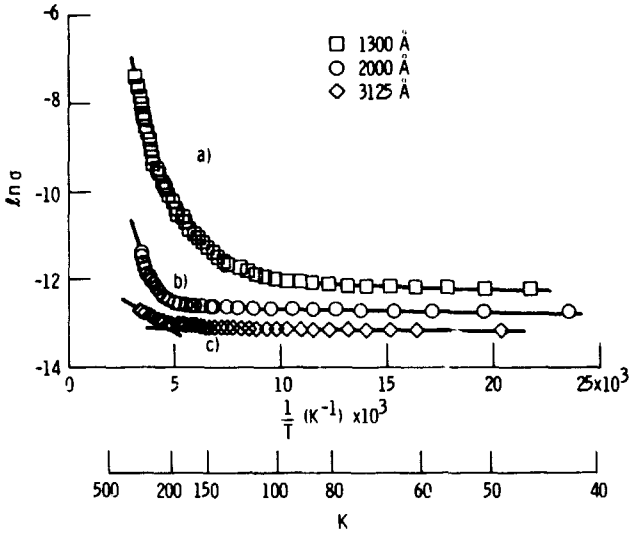


Figure 11. - Plot of the natural logarithm of the conductivity vs reciprocal temperature for three different ZnTe films of varying thickness. Curve (a) is for a 1300 Å thick film, curve (b) is for a 2000 Å thick film, and curve (c) is for a 3125 Å thick film.

| 1. Report No. | 2. Government Accession No. | 3. Recipient's Catalog No. |
|---|---|---|
| NASA TM-87119 | | |

| 4. Title and Subtitle | 5. Report Date |
|---|---|
| Ion Beam Sputter Deposited Zinc Telluride Films | |
| | 6. Performing Organization Code: 506-55-72 |
| 7. Author(s): Daniel A. Gulino | 8. Performing Organization Report No.: E-2726 |
| | 10. Work Unit No. |
| 9. Performing Organization Name and Address: National Aeronautics and Space Administration, Lewis Research Center, Cleveland, Ohio 44135 | 11. Contract or Grant No. |
| | 13. Type of Report and Period Covered: Technical Memorandum |
| 12. Sponsoring Agency Name and Address: National Aeronautics and Space Administration, Washington, D.C. 20546 | 14. Sponsoring Agency Code |

15. Supplementary Notes

Prepared for the 32nd National Symposium of the American Vacuum Society, Houston, Texas, November 18-22, 1985.

16. Abstract

Zinc telluride is of interest as a potential electronic device material, particularly as one component in an amorphous superlattice, which is a new class of interesting and potentially useful materials. This paper describes some structural and electronic properties of ZnTe films deposited by argon ion beam sputter deposition. Films (up to 3000 Å thick) were deposited from a ZnTe target. A beam energy of 1000 eV and a current density of 4 $mA/cm^2$ resulted in deposition rates of approximately 70 Å/min. The optical band gap was found to be approximately 1.1 eV, indicating an amorphous structure, as compared to a literature value of 2.26 eV for crystalline material. Intrinsic stress measurements showed a thickness dependence, varying from tensile for thicknesses below 850 Å to compressive for larger thicknesses. Room temperature conductivity measurements also showed a thickness dependence, with values ranging from $1.86 \times 10^{-6}$ $o\Omega^{-1}$ $cm^{-1}$ for a 300 Å film to $2.56 \times 10^{-1}$ $\Omega^{-1}$ $cm^{-1}$ for a 2600 Å film. Measurement of the temperature dependence of the conductivity for these films showed complicated behavior which was thickness dependent. Thinner films showed at least two distinct temperature dependent conductivity mechanisms, as described by a Mott-type model. Thicker films showed only one principal conductivity mechanism, similar to what might be expected for a material with more crystalline character.

| 17. Key Words (Suggested by Author(s)) | 18. Distribution Statement |
|---|---|
| Thin films; Amorphous semiconductors; Zinc telluride; Sputter deposition | Unclassified - unlimited<br>STAR Category 76 |

| 19. Security Classif. (of this report) | 20. Security Classif. (of this page) | 21. No. of pages | 22. Price* |
|---|---|---|---|
| Unclassified | Unclassified | | |

*For sale by the National Technical Information Service, Springfield, Virginia 22161